

# The EMI scanner and its application to clinical diagnosis

James V. Zelch, M.D.  
Paul M. Duchesneau, M.D.  
Thomas F. Meaney, M.D.  
Anthony F. Lalli, M.D.  
Ralph J. Alfidi, M.D.  
Margaret G. Zelch, M.D.

*Division of Radiology*

The concept of computer application to diagnosis by roentgenography has been studied by many investigators; however, the ultimate development and application of the process to clinical medicine is mainly the work of Ambrose and Hounsfield and EMI Ltd.<sup>1, 2</sup> The basic concept of utilizing digital computers to measure variations in x-ray absorption was tested by Ambrose, neuro-radiologist at Atkinson-Morley's Hospital, and was initially reported to the British Institute of Radiology in April 1972.<sup>1, 3</sup>

The EMI scanner has made it possible to analyze the depths of the brain without danger or discomfort to the patient, and to diagnose brain tumors, hydrocephalus, cerebral atrophy, and cerebral infarcts without contrast agents or radioactive material. This ingenious application of the computer permits analysis of the variations in x-ray absorption through multiple sections of brain substance. The picture produced displays the structure and configuration of the soft tissues of the brain. The unit installed at the Cleveland Clinic in January 1974 has been used in 450 cases. In general, the early experience here parallels that in other centers,<sup>3-5</sup> and it is apparent that computerized axial tomography (CAT) will have

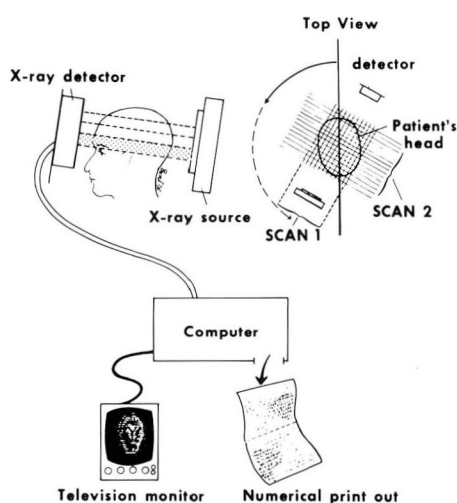


**Fig. 1.** Schematic diagram shows the basic principles of the EMI scanner. X-rays pass through the patient's head to a detector. The source and detector rotate around the head. The data are received by computer which calculates absorption values and provides a digital print-out and a cathode ray tube image.

a significant impact on the "usual" approach to the diagnosis and treatment of neurologic disorders.

### Technique

To describe the intricate computer technology and the mechanical structures of the unit is not the purpose of this report; a detailed description has been published.<sup>2, 6-9</sup> However, a basic understanding of the mechanisms involved is necessary to appreciate the extraordinary capabilities of the scanner.

The EMI system (*Fig. 1*) is an x-ray unit in the pure sense of the word, in that it emits photons that pass through the skull in a narrow beam to sensitive crystal detectors. The transmission of the x-ray photons can be measured and analyzed by a computer which demonstrates the internal architecture of the brain. The computer is programmed

to recover and analyze an enormous quantity of information heretofore lost by conventional roentgenography.<sup>2</sup> By solving equations of absorption coefficients, a display is produced on a cathode ray tube (CRT) which is a picture of the intervening brain tissues. A black and white record permits analysis of all densities from black (air) to white (bone) and permits Polaroid photography as a permanent record.

The system utilizes the principles of tomography and examines the head in a series of brain slices extending from the base of the skull to the top of the calvarium. A single passage of the x-ray beam results in two contiguous slices, A and B of approximately 1.3 cm in width (*Fig. 2*). The tomographic recording is caused by the fixed alignment of the sodium iodide crystals to the x-ray source and the movement of the source and detectors around the patient.

### Materials and method

The first 450 CAT scans at the Cleveland Clinic are the basis for this

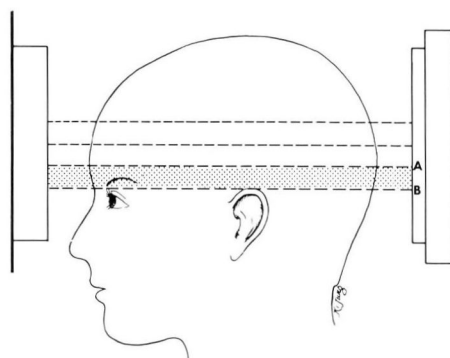


**Fig. 2.** Line drawing illustrates the plane and area of a typical scan (shaded areas). The detectors A and B permit recording of two contiguous slices.

report. Initially, attempts were made to obtain normal controls and patients with known pathologic diagnoses in an effort to conduct a meaningful clinical experiment. Because of clinical demands, within the first week this approach was not possible, and the cases reported here are an unselected cross section of neurologic practice. The majority of patients were referred from the Departments of Neurology and Neurosurgery; a significant number were referred from other clinical specialties and physicians outside the Cleveland Clinic. All scans were reviewed initially by one of us (P.M.D.) and again analyzed by another (J.V.Z.). The CRT display and Polaroid pictures provided the material for analysis of most patients. The digital print-out sheet was occasionally used to check density readings. A brief clinical impression was usually provided with a résumé of the neurologic findings available at the time of scan interpretation. The data presented are the initial interpretations of the scan and not the results of the review study. The clinical records and roentgenographic folds of all patients in this study were reviewed.

The patient lies comfortably on a

table with his head inserted into a firmly fitting adjustable rubber cap. The patient is positioned so that the plane of the slices is approximately 20° to 30° from the orbitomeatal line (Fig. 2). This makes possible the analysis of the orbits, base of skull, and posterior fossa in most patients. Subsequent scans are done at 2.5 cm intervals for three scans. A slit x-ray beam, approximately 2 cm in width, scans the head producing 160 readings of photon transmissions which are picked up by the crystal detectors. The gantry is indexed to transverse the head in 1° increments for 180°, thereby producing 28,800 (160 × 180) readings. The scanning time is approximately 5 minutes per slice with a measured radiation dose of 0.5 R.<sup>10</sup> This large number of readings from the crystal detectors-photo multiplier system is issued to the computer which solves simultaneous equations of absorption coefficients. By this means, the data produced by the individual brain elements in the course of the photon transit are measured and are unaffected by the tissue on either side. The digital printout is an accurate depiction of the densities displayed on the CRT. The CRT display is, in ef-

**Table 1.** Clinical data

Category	Presenting problems	Patients	Scans	Age			
				0-20	21-40	41-60	61-
1	Nonspecific	187	194	42	54	63	28
2	Dementia	53	54	8	0	18	27
3	Vascular	48	51	0	2	29	17
4	Metastatic	41	48	3	5	26	7
5	Suspected brain tumor	31	36	2	7	18	4
6	Postoperative follow-up	29	30	4	10	11	4
7	Orbit pathology	26	27	8	4	12	2
8	Trauma	10	10	2	5	2	1
Totals		425	450	69	87	179	90

Table 2. EMI diagnosis

Category	Presenting problems	Normal	En- larged spaces	Increased density	De- creased density	Bone defects	Totals
1	Nonspecific	156	10	14	14	0	194
2	Dementia	7	41	1	5	0	54
3	Vascular	15	5	4	27	0	51
4	Metastatic	17	1	6	20	4	48
5	Suspected brain tumor	14	0	16	6	0	36
6	Postoperative follow-up	11	6	10	3	0	30
7	Orbit pathology	16	0	8	3	0	27
8	Trauma	6	1	0	3	0	10
Totals		242	64	59	81	4	450

fect, a picture of the brain as depicted by matrix absorption coefficients and minified to one third of actual size.

Table 1 gives age grouping relative to clinical problems of the 425 patients. Twenty-five scans were repeated. The age range was from 3 months to 87 years. Category 1, nonspecific, includes patients with seizures, headaches, personality disorders, anxiety, and other vague complaints. Category 2, dementia, also includes nine retarded patients in the pediatric age group. Category 3, vascular, includes primarily patients with cerebral vascular insufficiency and "completed strokes." Acute cerebral hemorrhage, arteriovenous malformations, and intracerebral aneurysms are also included. Category 4 includes all patients with a known primary carcinoma outside the brain. Category 5 includes all patients whose clinical findings suggested a brain tumor. Lesions in or about the sella are included. Category 6, postoperative, includes patients evaluated for recurrence of tumor and patients who are undergoing treatment for a known disease. In Category 7 are patients referred from the Department of Ophthalmology because

of suspected specific abnormalities of the orbit and its contents. Category 8 includes all patients with recent trauma. Table 2 lists four large groups of diagnostic abnormalities in which the CAT findings correlated with the symptoms. Enlarged spaces indicate enlargement of the ventricular system or the subarachnoid spaces or both. Most patients in this group had either diffuse cerebral atrophy or hydrocephalus (normal pressure hydrocephalus). Increased density and decreased density indicate the appearance of an abnormal zone as related to the surrounding white and gray matter. A final group including bone defects was necessary for four patients with metastatic disease presenting as defects in the skull.

Results

Table 3 indicates the specific abnormalities detected in each of the eight categories. Of particular interest are patients with nonspecific complaints in whom seven tumors were detected. There were seven false positives and three false negatives. The false positives included two interpretations of mass density resulting from Panto-

paque droplets discovered on review of the plain films. Two additional cases of localized increased density were interpreted as tumor and diagnosed angiographically as cerebrovascular accidents. One malignant melanoma was misinterpreted as a cerebral infarct and two interpretations of subdural hematoma proved normal. No patient was subjected to a surgical procedure because of a false positive CAT scan. Three false negative interpretations were made: one large, parietal, occipital arteriovenous malformation was interpreted as normal, and two malignant brain tumors were missed. A review of the scan of the patient with arteriovenous malformation was again interpreted as normal. A retrospective analysis indicates that the two cases of brain tumors are positive beyond question, but were missed due to inexperience.

An attempt was made to correlate the CAT scans with plain skull films, isotope scans, cerebral angiography, pneumoencephalography, and pathologic findings. This study is continuing, but the data available at this time are not statistically significant. The major obstacle to this study has been the wide acceptance of the EMI diagnosis by the referring physicians. For the vast majority of patients with normal CAT scans, or scans showing atrophy or an area of devitalized brain, the results were accepted at face value, and the patient was not subjected to additional contrast studies. This study will continue, and the results will be reported when sufficient data are available.

## Discussion

CAT is producing a completely new dimension in the diagnosis of neuro-

logic disorders. The data in this report indicate the remarkable ability of the scanner to reproduce for analysis the internal structures of the brain. The rapid, almost uninhibited acceptance by physicians of this means of diagnosis is probably surpassed only by the acceptance of roentgenography in the late 19th century. The experience of the Cleveland Clinic, like that of other institutions possessing the EMI scanner, is wholly enthusiastic.

The CAT output and the actual cut section of the brain are remarkably similar (*Fig. 3*). Transverse axial scan pictures are viewed as though one were looking into the cranium from above, and like all other roentgenographic methods, the size, shape, and position of structures, such as the ventricles, pineal, and subarachnoid spaces are identified and studied. The accurate and reproducible pictures of brain substance allow for easy adjustment to the transverse axial anatomy.<sup>11</sup> The CAT scan in *Figure 3* should lay to rest any debate on whether computers are applicable to radiologic practice. The computer system is able to measure and separate attenuation of the beam by intervening tissues, and demonstrate the data in the many illustrations provided. All soft tissues of the brain fall within a narrow band of densities which in the past have been obscured by the superimposition of bone. No single method short of direct vision can give comparable information.

The system has two major drawbacks: (1) the patient must be able to lie perfectly still during the scanning sequence, and (2) there is a time delay of 5 to 10 minutes before viewing is possible. Eight patients in our study were excluded because of motion arti-



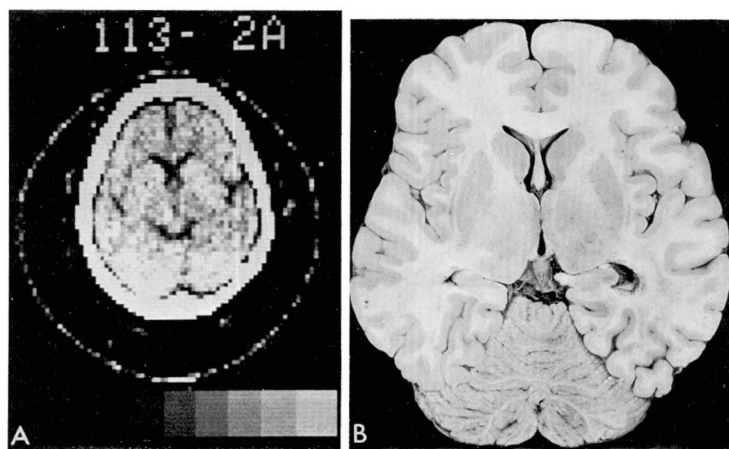


**Fig. 3.** A, *left*. CAT scan as seen on cathode ray tube. The skull is represented by the white outer zone with the subarachnoid spaces and a large computer artifact accounting for the black lining. The large gray areas are cortical tissue with lighter shades central representing the basal ganglia and internal capsule. Central dark zones are the ventricles and the subarachnoid cisterns. B, *right*. A tissue slice at the same level and angle ( $20^\circ$ ) demonstrates the actual anatomy for comparative analysis.

facts, and several procedures were cancelled because of poor cooperation. Two other areas of confusion occur when Pantopaque or air studies are carried out prior to the CAT scan. False positive interpretations for two patients were given because of the presence of Pantopaque in the subarachnoid spaces. Positioning of the patient requires a conscientious technician. For routine scanning, a  $20^\circ$  to  $30^\circ$  angulation from the orbitomeatal line is selected to visualize the orbits as well as the structures in the posterior fossa. This angulation is not rigid and we do attempt to tailor the scanning procedure to the suspected area of pathology. For orbital lesions, the initial CAT slices are obtained by a beam directed along the orbitomeatal line with subsequent scans angled to  $30^\circ$ .

An accurate diagnosis of brain tumor without the use of contrast agents and without danger or discomfort to the patient was made in 57 proven

cases and a probable diagnosis in an additional 18 (*Table 3*). Brain tumors appear as areas of abnormal density which distort the normal morphology of the brain. The same roentgenographic principles that apply to other diagnostic modalities are applicable to the CAT scan; namely, the presence of a density change compared to surrounding normal tissues, displacement of structures (ventricles, pineal gland, choroid plexus) and sequelae (hydrocephalus, bone defects). Although it has been our experience that the CAT scan is precise and accurate in its delineation of pathologic lesions, we are presently unable to correlate the scan abnormalities with the histology of brain tumors. Perhaps when the immense experience on a worldwide basis is tabulated, pathognomonic patterns will emerge. Neoplastic lesions of the brain are represented as masses of diminished density in *Figure 4 A through C*, as masses of increased density in *Figure 5 A and B*, as masses

**Table 3. EMI results**

Category	Presenting problems	Tumor	CVA	Atrophy	Diagnosis (not confirmed)	Others*	False positive	False negative	Normal	Totals
1	Nonspecific complaints	7	2	16	7	2	4	0	156	194
2	Dementia	0	4	42	0	0	1	0	7	54
3	Vascular	3	27	5	0	0	0	1	15	51
4	Metastatic	14	0	1	12	4	0	0	17	48
5	Suspected brain tumor	18	0	0	2	0	0	2	14	36
6	Postoperative follow-up	8	0	7	4	0	0	0	11	30
7	Orbit pathology	7	0	0	3	1	0	0	16	27
8	Trauma	0	0	0	0	2	2	0	6	10
Totals		57	33	71	28	9	7	3	242	450

\* Subdural hematoma, bone lesion, congenital anomalies, aneurysm.

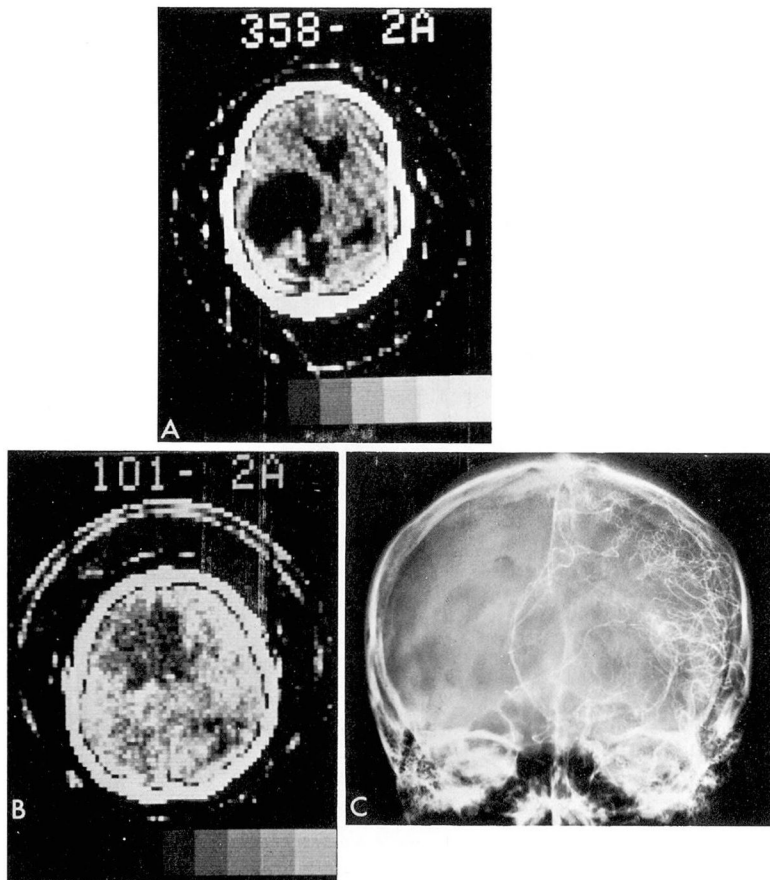


**Fig. 4.** A, *top*. Dermoid tumor. A 41-year-old patient with seizure disorder has a large area of diminished density on the left. B, *bottom left*. Astrocytoma of the left frontal lobe in a 21-year-old patient with left-sided headaches. The CAT scan shows a large area of diminished density. C, *bottom right*. Left carotid angiogram in the same patient. Anteroposterior view shows round shift of anterior cerebrals from frontal tumor.

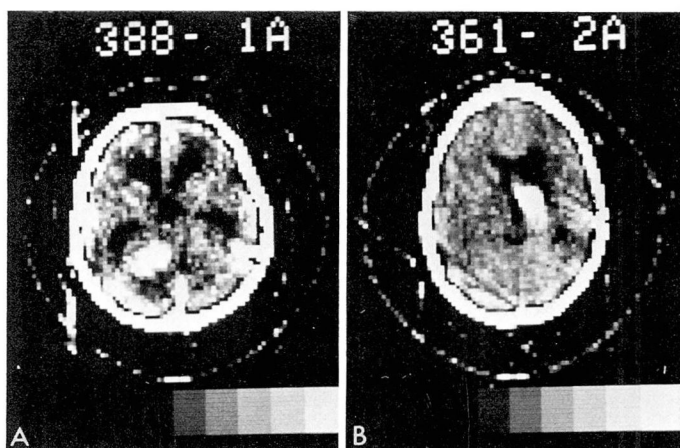


**Fig. 5.** High density tumors. A, *left*. Acoustic neuroma. CAT scan in a patient with vertigo shows a dense tumor of left cerebellopontine angle. B, *right*. Meningioma. CAT scan of 11-year-old with a meningioma of the floor of the right middle fossa.

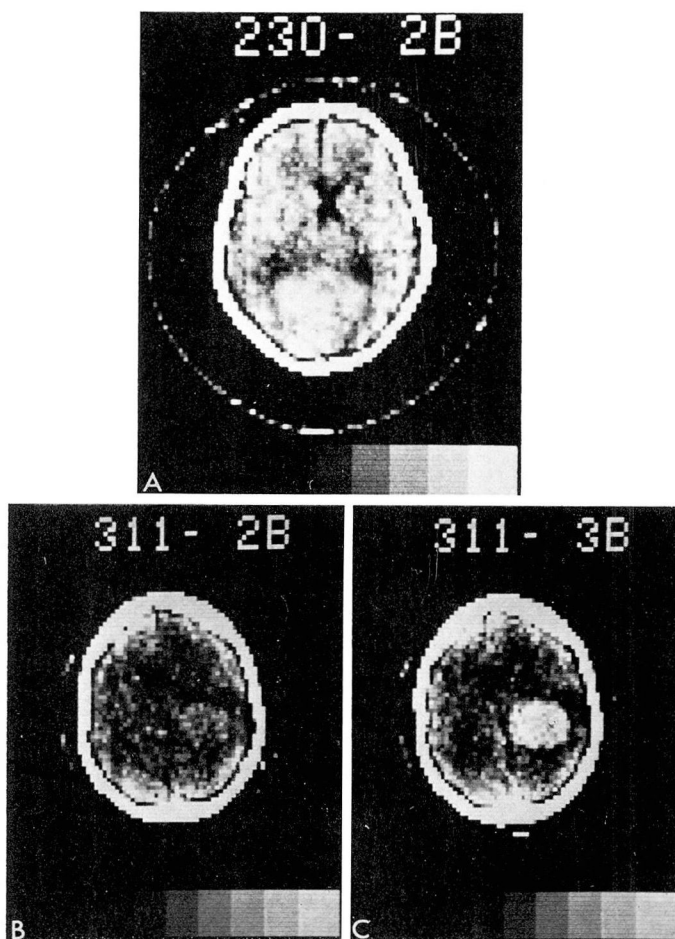


**Fig 6.** A, *top*. Metastatic rhabdomyosarcoma. CAT scan of a 10-year-old girl with signs of tentorial herniation shows a large posterior parietal zone of slightly increased density. B, *bottom left*. CAT scan of patient with meningioma with only faint visualization of an area of slight density change. C, *bottom right*. In the same patient, the area of density change is accentuated by the administration of a contrast agent.



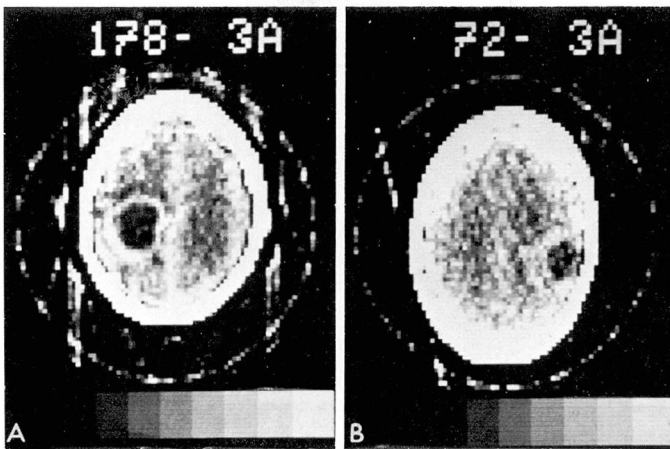


**Fig. 7.** Cystic tumors. A, *left*. Astrocytoma of the left parietal lobe in a 74-year-old patient with acute right hemiparesis. B, *right*. Meningioma with central cavitation in a 58-year-old patient.



**Fig. 8.** A CAT scan in a patient with a posterior fossa astrocytoma showing a mass of increased density causing hydrocephalus.

of density similar to that of surrounding brain tissues in *Figure 6 A through C*. Brain tumors can appear cystic (*Fig. 7A and B*) and cause distortion of the normal structures (*Fig. 8*). Most mass lesions clearly show displacement of ventricles and are diagnosed with a high level of confidence. All surgically proven neoplasms were demonstrated

on CAT scans. Two of 57 (3.5%) were incorrectly interpreted as normal. Our experience includes three tumors visualized only with contrast enhancement, and it has become our practice to administer routinely 40 to 50 ml of contrast medium before the examination of patients suspected of having brain tumors. There has been concern about obscuring low density tumors by this practice; however, no example of this is available.

Confirmation of a clinical diagnosis of dementia is an important application of the CAT scans. The cerebrospinal fluid spaces are readily visible on the scan and patients with dilated ventricles and dilated subarachnoid spaces of the convexities can easily be separated from those that are normal. This method allows for easy and safe evaluation of patients suffering from progressive neurologic deficits and can exclude mass lesions or vascular insults as the cause of their symptoms. The almost instant acceptance of this mode of diagnosis in these patients is testimony to its value. Few patients in

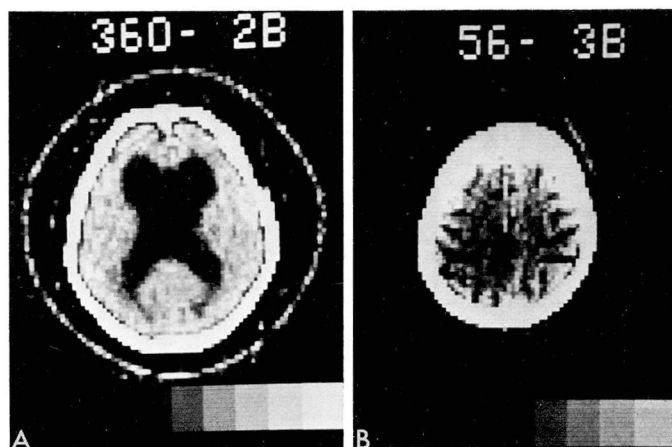


**Fig. 9.** A, *left*. Patient with dementia has a large ventricular system, but no evidence of increase in the subarachnoid spaces (normal pressure hydrocephalus). B, *right*. Patient with similar complaints of dementia is found to have large sulci indicative of generalized cerebral atrophy.

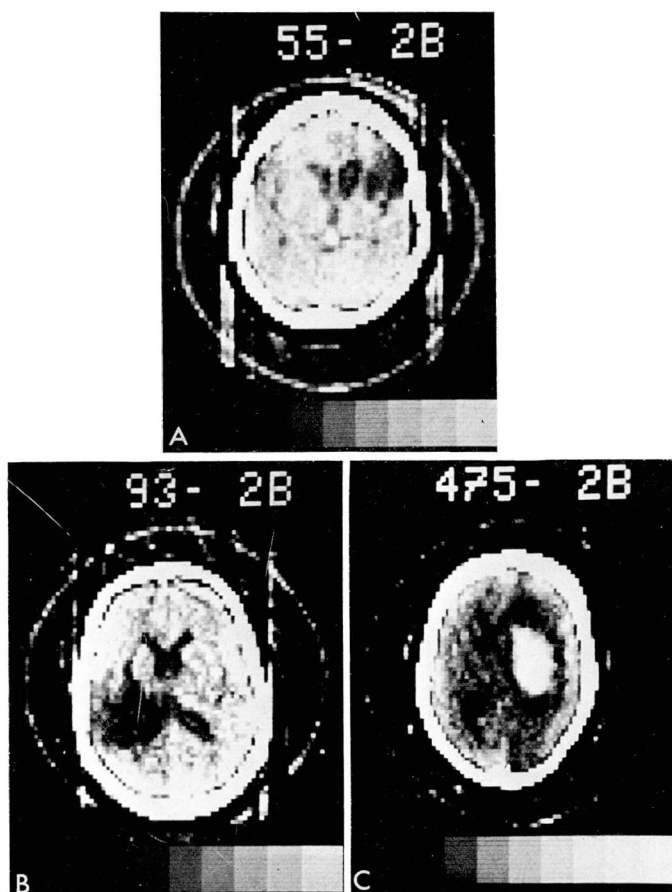


**Fig. 10.** Cerebrovascular accidents. A, *top*. Patient with a past history of transient ischemic attacks has a zone of diminished density in the right frontal area associated with dilatation of the frontal horn of the right lateral ventricle. B, *bottom left*. A CAT scan in a patient with acute onset of left hemiparesis shows a large area of infarct in the left parietal lobe. C, *bottom right*. Patient with evidence of an acute CVA has a broad zone of increased density characteristic of a cerebral hemorrhage.

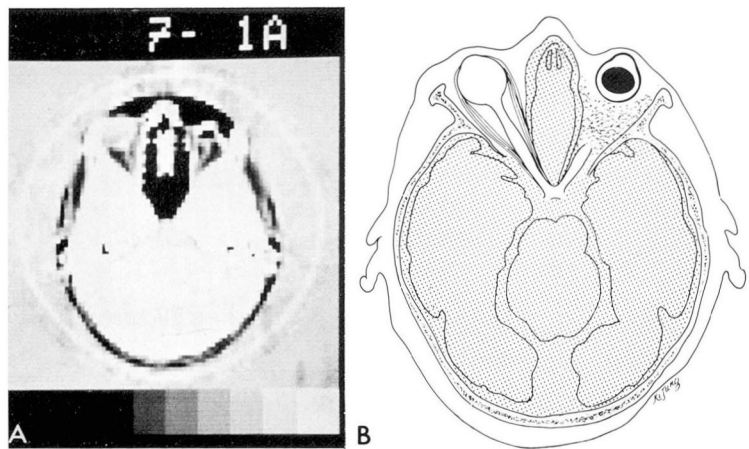


**Fig. 11.** Orbital views. A, left. CAT scan of a normal left eye with the optic nerve and globe visualized. B, right. Drawing shows the prosthesis in the right eye.

this category have undergone encephalography to confirm the presence of hydrocephalus or atrophy and only one radio-iodinated serum albumin (RISA) scan has been performed. Visualization of the ventricular system in the diagnosis of hydrocephalus is easily made. The wide variance in appearance between normal pressure hydrocephalus (*Fig. 9A*) and diffuse cerebral atrophy (*Fig. 9B*) is demonstrated. It has been difficult to justify the risk of additional procedures with the information available from CAT scans. In 42 of the 53 patients, the diagnosis of atrophy or hydrocephalus was confirmed. CAT scans will probably become the procedure of choice in this category (*Table 3*).

The CAT scan offers help in four areas related to cerebrovascular disease: (1) confirming the diagnosis and assessing the area of damage, (2) determining the location and extent of cerebral hemorrhage, (3) excluding other possible causes of the symptoms, and (4) analyzing the sequelae.

The diagnosis of cerebrovascular disease was confirmed in 27 of 41 pa-

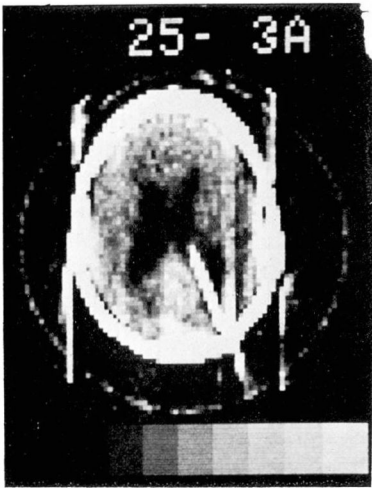


**Fig. 12.** Shunted hydrocephalus. A CAT scan demonstrating moderate dilatation of the ventricular system and a shunt catheter in the right lateral ventricle.

tients. Three unsuspected tumors and five cases of cerebral atrophy were discovered. The CAT scan also provides a picture of the effects of the vascular insult on cerebral tissue. The area of devitalized brain is usually seen as a zone of diminished density, with the ventricular system pulled toward the infarct and minimally dilated (*Fig.*

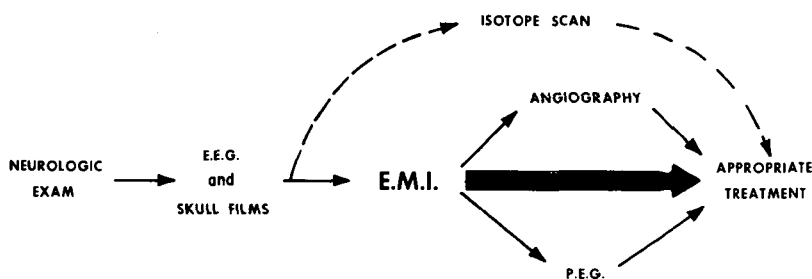


**Fig. 13.** Schematic representation of the place of the EMI scan in the diagnosis of neurologic disorders.

10A and B). An area of increased density in patients suspected of CVA indicates an organized hematoma (Fig. 10C).

A major advance in the diagnosis of orbital pathology has been observed. Figure 11A and B shows the normal orbit with optic nerve and globe on the left and a sectioned optic nerve with prosthesis on the right. The accompanying diagram emphasizes the important findings. Seven orbital tumors have been demonstrated in this group with an additional three probable but not confirmed. In the past the diagnosis of such lesions has eluded all but the most sophisticated roentgenographic methods.

The large group of patients with suspected metastasis to the brain and those with known tumors who are undergoing therapy or being evaluated for recurrence have been analyzed to evaluate the extent of disease or progress of therapy. Figure 12 is an example of shunted hydrocephalus to be followed by interval CAT scans.

The EMI scanner has secured a place in neurodiagnosis (Fig. 13). It is natural to inquire whether the CAT scans will replace conventional roentgenography and who should have the procedure. At present these questions are left to the discretion of the refer-

ring physician. However, it is believed that definite recommendations will be forthcoming in the immediate future. The material is presented to introduce the readers to a powerful new weapon which has been added to the diagnostic armamentarium of the radiologists. This will undoubtedly alter significantly the practice of neuroradiology.

### Summary

The EMI scanner is unsurpassed in recent developments in radiology and may prove worthy of recognition second only to the discovery of x-rays. The machine provides highly accurate data which are displayed as recognizable structures. It approaches the ideal diagnostic unit, in that it is fast, accurate, and safe. For these reasons and others, it is attractive to both the physician and the patient. We have entered a new era of x-ray capabilities.

### References

1. Ambrose J, Hounsfield G: Computerized transverse axial tomography. *Br J Radiol* 46: 148-149, 1973.
2. Hounsfield GN: Computerized transverse axial scanning (tomography). Part 1. Description of system. *Br J Radiol* 46: 1016-1022, 1973.
3. Ambrose J: Computerized transverse axial scanning (tomography). Part 2. Clinical application. *Br J Radiol* 46: 1023-1047, 1973.



4. Baker HL, Campbell JK, Houser DW, et al: Computer assisted tomography of the head; an early evaluation. *Mayo Clin Proc* 49: 17-27, 1974.
5. New PFJ, Scott WR, Schnur JA, et al: Computerized axial tomography with the EMI Scanner. *Radiology* 110: 109-123, 1974.
6. Fischgold H: L'EMI-Scanner. *J Radiol Electrol Med Nucl* 54: 1-5, 1973.
7. Ommaya AK: Computerized axial tomography of the head; the EMI Scanner, a new device for direct examination of the brain "in vivo." *Surg Neurol* 1: 217-222, 1973.
8. Peters TM, Smith PR, Gibson RD: Computer aided transverse body-section radiography. *Br J Radiol* 46: 314-317, 1973.
9. Technology Review: x-ray diagnosis peers inside the brain. *New Scientist* 54: 207, 1972.
10. Perry BJ, Bridges C: Computerized transverse axial scanning (tomography). Part 3. Radiation dose considerations. *Br J Radiol* 46: 1048-1051, 1973.
11. Potter GD: *Sectional Anatomy and Tomography of the Head; an Atlas of the Normal Sectional Anatomy of the Head*. New York, Grune and Stratton, Inc., 1971.